LEVEL II

DNA 5503F

CONTINUED PERFORMANCE OF THE WIDEBAND SATELLITE EXPERIMENT

Charles L. Rino
Robert C. Livingston
Boyd C. Foir
Michael D. Cousins
SRI International
333 Ravenswood Avenue
Menlo Park, California 94025

31 Jan [redacted] 81

51

Final Report, [redacted] 1 Jun [redacted] 77–31 Jan [redacted] 81

CONTRACT No. DNA 001-77-C-0220

APPROVED FOR PUBLIC RELEASE;
DISTRIBUTION UNLIMITED.

THIS WORK SPONSORED BY THE DEFENSE NUCLEAR AGENCY
UNDER RDT&E RMSS CODE B322077462 I25AAXHX63340 H2590D.

Prepared for
Director
DEFENSE NUCLEAR AGENCY
Washington, D. C. 20305

Destroy this report when it is no longer needed. Do not return to sender.

PLEASE NOTIFY THE DEFENSE NUCLEAR AGENCY, ATTN: STTI, WASHINGTON, D.C. 20305, IF YOUR ADDRESS IS INCORRECT, IF YOU WISH TO BE DELETED FROM THE DISTRIBUTION LIST, OR IF THE ADDRESSEE IS NO LONGER EMPLOYED BY YOUR ORGANIZATION.

UNCLASSIFIED

SECURITY CLASSIFICATION OF THIS PAGE (When Data Entered)

REPORT DOCUMENTATION PAGE	READ INSTRUCTIONS BEFORE COMPLETING FORM
1. REPORT NUMBER: DNA 5503F	2. GOVT ACCESSION NO.: AD-A099 819
3. RECIPIENT'S CATALOG NUMBER:	
4. TITLE (and Subtitle): CONTINUED PERFORMANCE OF THE WIDEBAND SATELLITE EXPERIMENT	5. TYPE OF REPORT & PERIOD COVERED: Final Report for Period 1 Jun 77 - 31 Jan 81
	6. PERFORMING ORG. REPORT NUMBER: SRI Project 6434
7. AUTHOR(s): Charles L. Rino, Boyd C. Fair, Robert C. Livingston, Michael D. Cousins	8. CONTRACT OR GRANT NUMBER(s): DNA 001-77-C-0220
9. PERFORMING ORGANIZATION NAME AND ADDRESS: SRI International, 333 Ravenswood Avenue, Menlo Park, California 94025	10. PROGRAM ELEMENT, PROJECT, TASK AREA & WORK UNIT NUMBERS: Subtask I25AAXHX633-40
11. CONTROLLING OFFICE NAME AND ADDRESS: Director, Defense Nuclear Agency, Washington, D.C. 20305	12. REPORT DATE: 31 January 1981
	13. NUMBER OF PAGES: 54
14. MONITORING AGENCY NAME & ADDRESS (if different from Controlling Office)	15. SECURITY CLASS (of this report): UNCLASSIFIED
	15a. DECLASSIFICATION/DOWNGRADING SCHEDULE: N/A

16. DISTRIBUTION STATEMENT (of this Report)

Approved for public release; distribution unlimited.

17. DISTRIBUTION STATEMENT (of the abstract entered in Block 20, if different from Report)

18. SUPPLEMENTARY NOTES

This work sponsored by the Defense Nuclear Agency under RDT&E RMSS Code B322077462 I25AAXHX63340 H2590D.

19. KEY WORDS (Continue on reverse side if necessary and identify by block number)

Propagation Theory
Radio Waves
Scintillation
Wideband Satellite

20. ABSTRACT (Continue on reverse side if necessary and identify by block number)

This report summarizes the work completed during the active data-taking phase of the Wideband Satellite Program. The report includes a complete description of the Wideband satellite data base and a summary of the accomplishments of the program in the areas of propagation theory, channel modeling, and the structure and development of the naturally-occurring ionospheric irregularities that cause scintillation. A complete bibliography is included.

DD FORM 1 JAN 73 1473 EDITION OF 1 NOV 65 IS OBSOLETE

UNCLASSIFIED

SECURITY CLASSIFICATION OF THIS PAGE (When Data Entered)

SUMMARY

This report formally completes the active data-taking phase of the Wideband Satellite Program. The experiment has been an outstanding success, both in meeting its objectives and in revealing several new and unexpected aspects of the structure of naturally-occurring ionospheric irregularities.

The report summarizes the extensive data base that was accumulated and processed during the three years of operation of the Wideband satellite. The data base is itself a unique and invaluable resource, because the Wideband satellite is the only experiment that has permitted completely unambiguous multifrequency phase-and-amplitude scintillation measurements.

The report outlines, in two categories, the major accomplishments of the Wideband satellite experiment. The first category has to do with propagation theory and channel modeling, which is the basis for extrapolating the Wideband satellite results to the disturbed nuclear environment (Section I). In this area the Wideband satellite program has stimulated a number of refinements in the propagation theory (Section II). The second category is the structure and development of the naturally occurring ionospheric irregularities that cause the scintillations. Here several unexpected and important new results have emerged (Section III).

This report is primarily a survey of the direct and related work that has resulted from the Wideband Satellite Program. A bibliography of the numerous reports, papers, and complementary efforts up to the time this report was written are included.

TABLE OF CONTENTS

LIST OF ILLUSTRATIONS

LIST OF TABLES

I INTRODUCTION

The Wideband Satellite Program formally started in 1968, when SRI International was awarded a contract to develop a satellite-borne, multi-frequency, phase-coherent beacon for measuring the propagation characteristics of the transionospheric channel. Radar propagation effects were the dominant concern at the time. Of particular interest was the determination of the maximum bandwidth signals that the disturbed ionosphere could support. A comb of seven equally-spaced UHF frequencies covering a 70-MHz bandwidth was, therefore, incorporated into the beacon for coherence-bandwidth measurements.

From the outset of the project, a formal channel-modeling approach was pursued. The ionosphere, insofar as the transmission of radio waves is concerned, is a linear medium. Because of this property, all propagation effects can be characterized in terms of a time-varying transfer function $h(t;f)$. The spatial structure of the perturbed wavefield is implicitly contained in the transfer function. The concept is illustrated in Figure 1.

One applies the channel model in the following manner: If a signal

$$S_i(t) = \mathrm{Re}\left\{v_i(t)\ \exp\left[2\pi i f_c t\right]\right\} \tag{1}$$

is transmitted, the received signal, $S_o(t)$, admits a representation similar to Eq. (1) with $v_i(t)$ replaced by

$$v_o(t) = \int \hat{v}_i(f)\ h\ (t;\ f + f_c)\ \exp\left[2\pi i f t\right]\ df \quad . \tag{2}$$

In (2) $\hat{v}_i(f)$--the fourier transform of $v_i(t)$--occupies a finite band of frequencies, B, such that $B/f_c \ll 1$. It is clear from (2) that if a sinusoidal signal for which $\hat{v}_i(f) = \delta(f)$ is transmitted, then the complex modulation imparted to $S_o(t)$ is $h(t;f_c)$. By using the phase-coherent

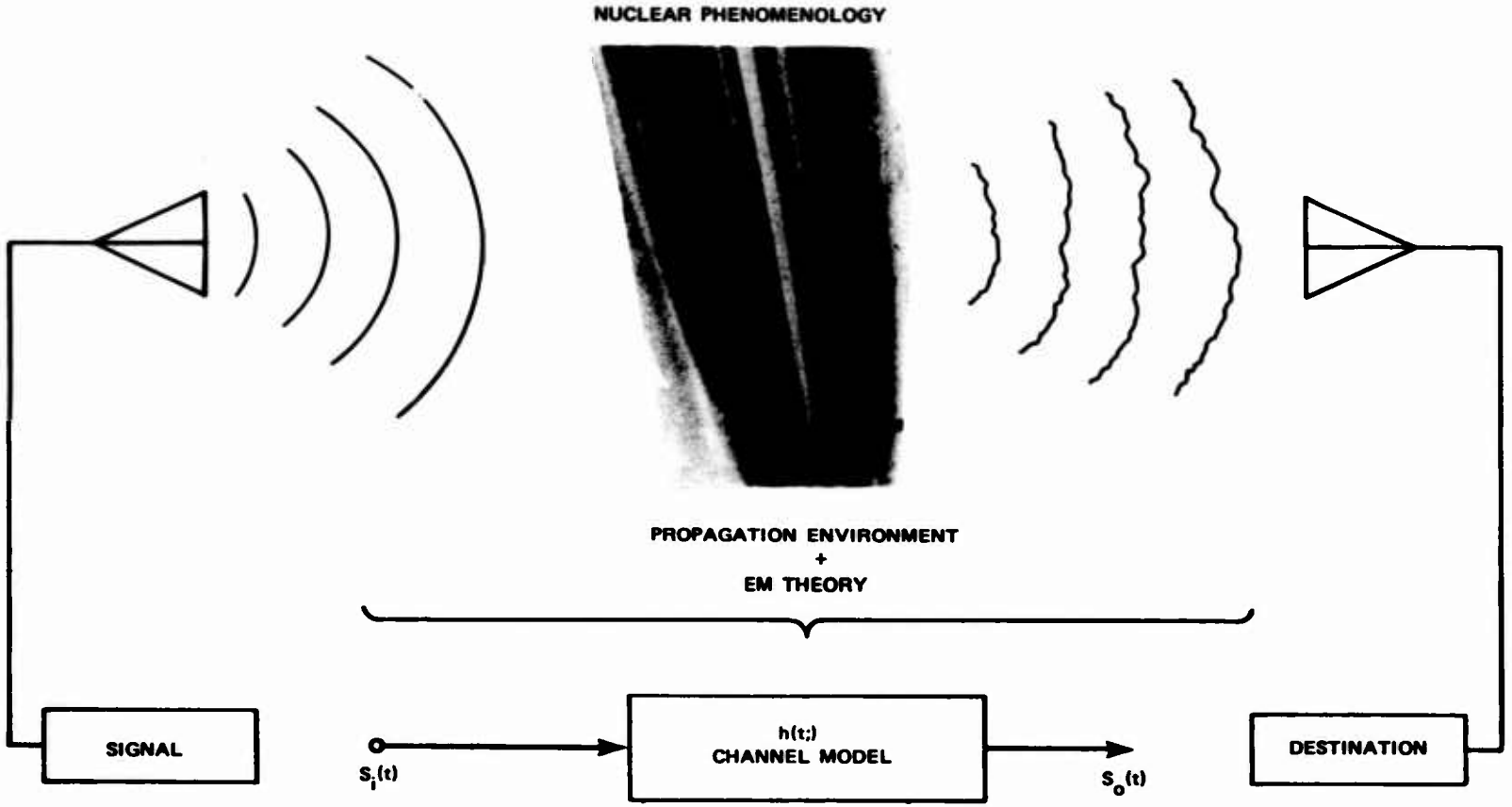

FIGURE 1 EQUIVALENT CHANNEL MODEL FOR IONOSPHERIC PROPAGATION EFFECTS

signal at S-band as a phase reference, the synchronously demodulated Wideband signal gives the complex signal $v_i(t) = h(t;f_c)$, which is the most basic quantity that is used in analyzing fading channels [see for example, Schwartz, Benet, and Stein, Communication Systems and Techniques, Ch. 9 (McGraw-Hill Book Co., 1966); and Kennedy, Fading Dispersive Communication Channels (John Wiley and Sons, Inc., 1969)].

Because h(t;f) cannot be predicted in detail, a statistical characterization must be used, although for most engineering applications a complete statistical description is unnecessary. Indeed, under conditions of Rayleigh fading, only second-order temporal and frequency coherence measures need be specified. An appropriate measure of the perturbation level is first used to estimate the onset of Rayleigh fading. The application of such a channel model for evaluating the performance degradation in communication or navigation systems is illustrated in Figure 2.

In principle, the problem is amenable to complete mathematical treatment. To accommodate all the complexities of various systems, however, simulations are invariably used. To faithfully reproduce the statistics of h(t;f), the diffraction process itself must be modeled. It is obviously more efficient, however, to directly generate a Gaussian process that has the same temporal and frequency coherence as h(t;f). The diffraction theory then has to supply only the second-order coherence measures and their geometrical dependence.

The Wideband satellite data base is ideally suited for testing both propagation theory simulations and the alternative Gaussian implementation. In the course of fulfilling this objective, moreover, the Wideband satellite experiment has provided invaluable information on the occurrence and structure of the striations that cause the propagation disturbances.

In this final report, which concludes the active data-taking phase of the Wideband Satellite Program, we review the major accomplishments of the program. In Section II the data base, acquired during the three years of continuous operation of the Wideband satellite, is summarized. The data have all undergone preliminary and summary analysis and are

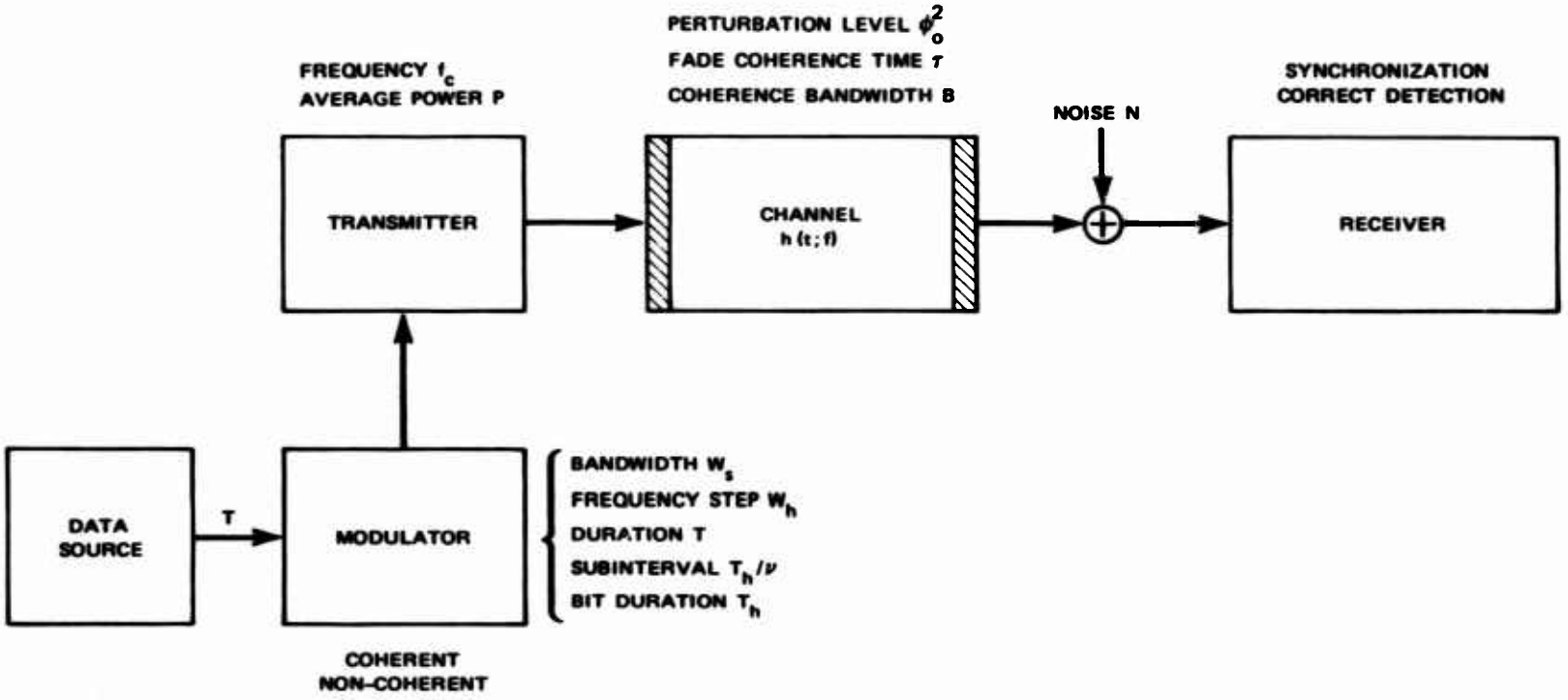

FIGURE 2 CHANNEL MODEL APPLICATION FOR COMMUNICATION AND NAVIGATION SYSTEMS

archived in a data library. This task is complete, and has provided a unique resource that can be productively utilized for many years to come.

In Section III, we review the accomplishments of the Wideband Satellite Program in the area of propagation theory and channel modeling. As noted in the Introduction, this effort was the major objective of the program. It has, moreover, resulted in a number of essentially new theoretical results concerning the propagation of radio waves in randomly irregular, power-law media.

In Section IV, we review the accomplishments of the Wideband Satellite Program in the area of irregularity occurrence, intensity, and structure. Here, as in the case of the propagation theory, a number of new and unexpected findings have developed. To provide a complete up-to-date summary, we have referenced the work performed under separate contracts, as well as new results that have emerged since the formal stop-work date for this contract.

In Section V, the operation of the DNA002 satellite beacon, up until its loss in August 1979 (caused by a boost-regulator circuit failure) is reviewed.

II THE WIDEBAND SATELLITE DATA BASE

The locations of the Wideband receiving stations are listed in Table 1. The Stanford station was moved to Kwajalein in October 1978 to provide data on the longitudinal variation of equatorial scintillation. Both the Poker Flat and the Kwajalein stations have three UHF phase-coherent remote antennas with a 900-m geomagnetic north-south baseline and a 300-m and a 600-m geomagnetic east-west baseline. The data accumulated during the active data-taking phase of the Wideband Satellite Program are summarized in Table 2.

For each pass, which provides ~ 15 min of data, a maximum of 13 complex channels are sampled (at a 500-Hz rate) and digitally recorded on 9-track tape (at 1600 bpi). The first step in the routine data reduction is to detrend the S band, the L band, the two extreme and center UHF channels, the 900-m, 600-m, and 300-m spaced-receiver channels, and the VHF channel (9 of the 12 recorded channels). The detrend cutoff is 0.1 Hz (10 s) and the detrended intensity and phase data for these nine channels are recorded at a 100-Hz rate. A continuous phase trend is preserved, together with the signal intensity trend, at a 20-Hz rate.

The detrended data are then processed to extract phase-and-amplitude scintillation indices, space and frequency correlation coefficients, and the spectral characteristics of the VHF and center UHF scintillation data. Summary parameters are computed for every 20-s data segment and recorded, together with satellite location and propagation geometry, at E- and F-region reference altitudes. These summary parameters, together with the intensity-and-phase trends for each of the routinely detrended channels, are preserved on summary tapes. A detailed description of the detrend and summary data is presented in Appendix A.

The routine processing described above has been performed on all of the data listed in Table 2. The detrend and summary tapes for all data are cataloged and stored in a data library at SRI International. These

Table 1

WIDEBAND GROUND STATIONS

Station	Latitude	Longitude	Dip Latitude
Poker Flat, Alaska	65°7'N	147°29'W	65.4°N
Stanford, California	37°24'N	122°10'W	42.8°N
Ancon, Peru	11°46'S	77°9'W	0.4°N
Kwajalein, Marshall Islands	9°24'N	16?°28'E	4.4°N

data have formed the basis for a number of scintillation morphology and propagation studies, which we shall describe in Sections III and IV. A more detailed discussion of the summary processing can be found in Fremouw et al. (1978).

In addition to the routine summary processing, several more elaborate data analysis procedures have been developed. To process the spaced receiver data, for example, all possible complex correlations among the four receivers must be computed. To accommodate this data load economically, an array processor was used. Preliminary results are described in Topical Report 1. Table 3 lists the passes that have been processed for spatial coherence studies.

For analysis of strong scatter effects, the L-band, the center UHF, and the VHF data from a selected subset of the most disturbed passes at Ancon and Kwajalein were detrended by using a 0.04 Hz (25 s) low-pass filter and a 250-Hz sample rate. Finally, the 7 UHF channels from the same data set have been separately detrended at 0.1 Hz for coherence bandwidth studies.

Selected subsets of the Poker Flat, Stanford, Kwajalein, and Ancon data have undergone a dual detrending procedure that separates the scintilation into fast and slow multiplicative components. This processing procedure was developed for analyzing the first-order signal statistics.

Table 2

SUMMARY OF WIDEBAND SATELLITE DATA BASE

May 1976 to August 1979

Poker Flat (1140 Passes)	
Regular Weekly Operations	
28 May 1976 to 25 May 1978	
10 July 1978 to 2 February 1979	
Intensive Campaign Operations	
13 to 16 November 1976	~ 40 passes*
7 to 17 November 1977	~ 48 passes*
28 February to 9 March 1978	~ 53 passes
28 November to 14 December 1978	~ 86 passes
27 January to 2 February 1979	~ 33 passes
Ancon (500 Passes)	
Regular Weekly Operations	
26 May 1976 to 17 June 1976	
8 July 1976 to 26 November 1977	
28 December 1977 to 15 April 1978	
19 September 1978 to 27 April 1979	
Intensive Campaign Operations	
8 March to 2 April 1977	~ 55 passes
28 February to 17 March 1978	~ 27 passes
Kwajalein (530 Passes)	
Regular Weekly Operations	
13 October to 22 December 1976	
5 January to 27 October 1977	
29 March to 28 August 1978	
Intensive Campaign Operations	
17 August to 30 September 1977	~ 85 passes
28 July to 29 August 1978	~ 50 passes
10 June to 3 August 1979	~ 40 passes
Stanford (100 Passes)	
Regular Weekly Operations	
26 May to 10 September 1976 (Site moved to Kwajalein October 1976)	

*Remote station operated at Fort Yukon, Alaska 5 to 18 November 1977.

Table 3

SPACED RECEIVER DATA ANALYSIS SUMMARY

Inclusive Dates	Passes	Books
Poker Flat		
February-July 1978	~ 180	50, 51, 52, 53*
Kwajalein		
June-July 1977 June-July 1978	~ 100	26, 49, 58

*Detrended only.

III PROPAGATION THEORY

A. First-Order Signal Statistics

The first-order statistics of radio-wave and light-wave scintillation have been the source of controversy since the first papers on the subject were published [see Rino (1980a)]. All attempts to rigorously justify either the log-normal or Gaussian models, including the Gaussian Rayleigh limit under conditions of strong scatter, have failed. The Wideband satellite data have consistently shown that scintillating signals are dominated by slow, trend-like phase variations even under conditions of strong scatter. The quadrature signal components are, therefore, never completely uncorrelated, as required by the Rayleigh and Rice models; moreover, the phase structure is not strictly Gaussian, as required by the log-normal model.

To accommodate the slow phase trends formally, Fremouw et al. (1976) postulated a multiplicative, two-component model. The most rapid complex signal scintillations are represented by a general Gaussian model. The slow-phase and associated amplitude variations are represented by a log-normal process. The partitioning, however, is somewhat arbitrary.

Fremouw et al. (1980) performed detailed tests of the two-component model, using Wideband satellite data. They showed that the most rapid scintillations can always be well represented by the general Gaussian model. The intermediate multiplicative component does not adhere so closely to the log-normal model. The best overall fits to the measured complex signal statistics were nonetheless obtained by using the two-component model. For intensity only, however, the Nakagami distribution (which includes the Rayleigh distribution as a special case) gives the best fit when tested against the two-component, general Gaussian, and log-normal models.

The two-component model has been used in both purely theoretical analysis [Johnson and Rino (1979)] and simulations [Scott and Knepp (1978)] of digital communications systems. Insofar as communication systems are concerned, the subtle departures of the signal statistics from the Gaussian model, in particular deviations from the Rayleigh limit, are unimportant. The slow trend-like phase variations, however, have important ramifications in the propagation theory.

B. Propagation Theory in Power-Law Environments

An early finding in the Wideband satellite data, also noted earlier in TRANSIT satellite differential phase data by Crane (1976), was that the value of the rms phase depends on the interval over which it is measured. This is easily understood in light of the fact that the phase spectral-density function has the power-law form

$$\varphi(f) \sim Tf^{-p} \tag{3}$$

where f is temporal frequency, T is the spectral-strength parameter, and p is the spectral index.

For a data interval of length τ_c, the spectrum is effectively truncated at a frequency $f_c \sim \tau_c^{-1}$. In the routine Wideband data analysis, a detrend filter is applied that removes all spectral components below f_c. In any case, as long as Eq. (3) applies for $f \gtrsim f_c$, the rms phase can be calculated as

$$\sigma_{\delta\phi}^2 = 2 \int_{f_c}^{\infty} Tf^{-p}\, df$$

$$= \frac{2T}{p-1} f_c^{(p-1)} = \frac{2T}{p-1} \tau_c^{p-1} \tag{4}$$

For the routine Wideband summary analysis, f_c was chosen to represent the approximate minimum frequency that makes a significant contribution to the corresponding intensity scintillation. It is important to note,

however, that T and p do not depend on how they are measured, and that they therefore constitute a completely unambiguous characterization of the average phase structure.

The ramifications of the power-law continuum of scale sizes that characterize the ionospheric irregularities have been developed in a series of papers and reports [Rino (1979a,b,c; Rino (1980b,c)]. The theoretical computations show that, in a power-law environment where the outer scale is much larger than the Fresnel radius, the diffraction effects are critically dependent on the power-law index p.

If $p < 3$, for example, the mutual coherence function can be characterized independent of the rms phase level. The intensity scintillation index S_4, moreover, converges to unity under conditions of strong scatter, which is a necessary (but not sufficient) condition for Rayleigh statistics. Indeed, under the same conditions, there is a simple relation between the intensity correlation function and the mutual coherence function. If $p > 3$, however, these simple relations break down.

It is fortunate, therefore, that the Wideband satellite data have consistently given spectral p indices less than 3. The most recent results clearly show, as discussed in Section IV, that the spectral index varies systematically with changing perturbation strength.

The weak-scatter theory has been applied to the Wideband satellite data in Rino (1979a). We note that the angle dependence of the scintillation is particularly important for low orbiting satellites such as Wideband. The theory is developed in Rino and Fremouw (1977). The time structure of the scintillation as measured by Wideband is discussed in Rino and Owen (1980a). In particular, the strong-scatter dependence of the coherence time on the spectral index has been verified.

To analyze the spaced-receiver data, an elaborate analysis procedure was developed. With an appropriate angle-dependence theory, the method gives simultaneous estimates of the anisotropy and apparent drift of the diffraction pattern. The method and preliminary results are described in Rino and Livingston (1978). The results confirm the high

degree of the field-aligned anisotropy of the irregularities. There is, however, a second axis of elongation in the auroral zone (see Section IV).

The frequency coherence across the Wideband UHF comb of seven frequencies, spanning a 70-MHz bandwidth, has been analyzed and compared to theoretical predictions in Rino et al. (1980a). Good results are obtained when the signal is appropriately parameterized. The UHF comb has also been used to synthesize a narrow pulse and to measure the ionosphere-induced delay jitter. The results are in good agreement with model computations.

The Wideband satellite data, overall, are in excellent agreement with model computations that are based on a power-law phase screen with an outer scale dimension that is larger than the largest Fresnel radius of practical interest.

C. Channel Modeling

The Wideband satellite data have verified the accuracy of simple formulas that give a basic set of parameters for characterizing the average performance degradation in communication systems. These parameters include: (1) the intensity scintillation index S_4, which saturates near unity under strong scatter conditions, (2) the temporal coherence times for intensity, τ_I, and the complex signal, τ_V, and (3) a measure of the delay jitter induced by frequency decorrelation. Measures of angle-of-arrival jitter and Doppler spread are also available. A complete parameter specification has been described by Wittwer (1980).

The time structure of the intensity scintillation under conditions of both weak and strong scattering has been thoroughly analyzed by Rino and Owen (1980a). The coherence of the complex signal itself has not been directly measured. The coherence bandwidth formula and the delay-jitter estimate have been verified in Rino et al. (1980a). The analysis accommodates wave-front curvature as well as signal decorrelation along the propagation direction.

The overall characterization of average scintillation structure derived from the Wideband experiment completely validates the propagation

theory. One must, of course, have an appropriate characterization of the in-situ irregularity structure. A minimal characterization includes: (1) the effective turbulence level, (2) the power-law index, (3) the anisotropy of the irregularities, and (4) an effective height and thickness of an equivalent phase screen that reproduces the average signal structure. The propagation theory is therefore essentially complete.

IV IONOSPHERIC IRREGULARITY STRUCTURE AND OCCURRENCE

A. General Characteristics

The Wideband satellite phase scintillation data have consistently shown spectral indices [p in Eq. (3)] that are less than 3; moreover, the p index varies systematically with increasing perturbation strength. It has been found empirically that p follows a relationship of the form

$$p = p_o - \eta \log_{10} T \tag{5}$$

that p decreases as T increases. Because diffraction effects in the phase data should ultimately tend to cause the same effect, there was an initial reluctance to accept the result as genuinely reflecting the underlying irregularity structure.

In-situ data from the AE-E satellite, however, have shown exactly the same trend: for a one-dimensional in-situ spectral density function of the form $T_1 f^{-p_1}$, p_1 admits a functional dependence on T_1 of the form given by Eq. (5) with the same η parameter [Livingston et al. (1980)]. This behavior has also been confirmed in rocket probe data from a recent DNA equatorial spread-F campaign [Rino et al. (1980b)]. Recall that $p_1 = p - 1$; thus, if $p = 3$, then $p_1 = 2$.

As a final confirmation of the varying spectral index, we have accommodated Eq. (5) in the propagation theory. In doing so, a considerable improvement in the theoretical fits to intensity-coherence time data was obtained [Rino and Owen (1980b)]. The frequency coherence data clearly show evidence of a systematically varying spectral index [Rino et al. (1980a)].

The varying spectral index was an unexpected finding that has important ramifications. It had generally been accepted that a convective instability (e.g., gradient drift or Rayleigh-Taylor) generates striations with steep gradients (see Ossakow, 1979). Such an environment

would favor a k^{-2} one-dimensional in-situ spectral density function which implies p = 3. Equatorial and auroral irregularities that occur naturally are clearly much more complex.

In light of recent data from the DNA Kwajalein rocket campaign (PLUMEX), we believe that the steep gradients are broken up by the large-scale flow fields that develop in the course of the dynamic evolution of the background plasma. In the case of equatorial spread F, it is the depletions associated with backscatter plumes that generate the flow field. Appropriate simulations have not yet been performed to verify this conjecture, and a considerable amount of work needs to be done to understand all the ramifications of these new results.

B. High Latitude

The general morphology of the occurrence and latitudinal distribution of the auroral-zone scintillation, measured by the Wideband satellite, is described in [Rino and Matthews (1980)]. The most conspicuous feature in the data is a pronounced localized scintillation enhancement that occurs at the point where the propagation path to the satellite lies within a L shell [Fremouw et al. (1977)]. The unique localization of the enhancement has been shown to be caused by sheet-like irregularities--that is, irregularities that have a high degree of spatial coherence along L shells as well as along the magnetic field.

Other experiments have identified the source region to be localized in a latitudinally narrow enhanced F region [Rino and Owen (1980c); Vickrey et al. (1980)]. This particular scintillation phenomenon has received considerable attention from theoreticians [Ossakow and Chaturvedi (1978); Chaturvedi and Ossakow (1979)]. Field-aligned currents can destabilize a region, that might otherwise be stable, to the ordinary gradient drift instability. Both the mechanism and sheet-like structure of the irregularities are being intensely studied. The structure of scintillation, associated with auroral arcs and other general features of high-latitude scintillation as observed by Wideband, are discussed in [Rino et al. (1977)].

C. Equatorial

The occurrence and distribution of equatorial scintillation, as observed at Kwajalein in the north Pacific and Ancon, Peru, are described in [Livingston (1980)]. The most intense scintillation occurs at stations located near the geomagnetic equator. The occurrence at any given station, however, exhibits a strong seasonal dependence. The active period at Ancon persists for approximately 8 months, centered on December. At Kwajalein, the active period has a similar duration, but it is centered on July. Other stations report a pronounced seasonal dependence [see for example, Basu et al. (1980)].

The interrelationships among all the various manifestations of equatorial spread F are currently a subject of considerable interest, particularly in light of the results that have emerged from the recent DNA PLUMEX experiments. An invaluable contribution to that experiment was made by the ALTAIR radar which mapped the coherent backscatter, as well as making incoherent scatter measurements. This effort was partially supported under the Wideband program [Tsunoda et al. (1978), Topical Report 1].

The general subject of the total electron content (TEC) structure and its association with scintillation has not been treated under this contract. Some of the unique equatorial structures are described in [Rino et al. (1977)]. Work on both auroral and equatorial TEC structures are, however, currently being pursued under a separate contract.

V P76-5 SATELLITE

The design of the Wideband beacon dates back to the late 1960s. The experiment was originally designed (electrically and mechanically) to be compatible with the SAMSO P72-2 spacecraft built by the Rockwell Corporation. The P72-2 Satellite Program encountered many technical difficulties and scheduling delays before it finally suffered a launch failure in April 1975.

As part of the development program for the beacon, a prototype/spare flight beacon was constructed that was electrically and mechanically identical to the flight unit. With the launch failure of P72-2, discussions were held with DNA and SAMSO to determine what other, if any, launch opportunities existed. After many meetings, it was determined that one of the Navy spare TRANSIT spacecraft could be modified quickly and at a reasonable cost. Because the TRANSIT was designed to be launched on a Scout booster, the launch costs would be minimized.

In mid-1975, the Applied Physics Laboratory of John Hopkins University was awarded a contract to obtain a spare TRANSIT from the Navy, modify the spacecraft as necessary, and integrate the spare beacon for a launch on a Scout booster in 1976. This program was assigned the designation P76-5 by SAMSO. Two major modifications required by the TRANSIT spacecraft were (1) a new beacon antenna design, and (2) a boost regulator to raise the 10-VDC bus voltage to the 28 VDC required by the Wideband beacon. It is this boost regulator that most likely caused the recent failure of the Wideband satellite.

A major difference between the P72-2 and P76-5 program was the satellite orbit. Because the TRANSIT spacecraft carried only the Wideband experiment, the orbit could be optimized for that experiment. The satellite was launched into a precise noon-midnight, sun-synchronous orbit on 26 May 1976. The orbit was chosen to maximize the value of the data obtained; however, it is one of the worst possible orbits for the

hardware. Being in a noon-midnight orbit, the satellite passes through the earth's shadow on each orbit. This shadow time varies with the time of year, but averages about 35 minutes out of each 107-minute orbit. This repetitive encountering of the earth's shadow led to the first satellite power problem in June 1977.

A well known, but little understood, phenomena of nickel-cadmium batteries is the effect known as a "memory." The normal discharge curve for a ni-cad cell is a nearly constant voltage until the cell is completely discharged, followed by a sudden collapse in the terminal voltages. When a cell has been subjected to repeated partial discharges of the same magnitude, a memory develops within the cell. The discharge curve for a cell with memory departs from the normal discharge curve when the cell is repeatedly discharged below the depth previously reached. At that point, the terminal voltage drops to a lower plateau, where it remains until the cell is completely discharged. The lower bus voltage, resulting from the battery memory, caused the Wideband experiment to experience its first Low-Voltage Sense-Function (LVSF) shutdown in June 1977.

The LVSF is a special circuit incorporated into the boost regulator that was added to the original TRANSIT spacecraft. Its function is to prevent a catastrophic complete battery discharge. The LVSF monitors the buss voltage, and switches the boost regulator into a no-boost state when the buss voltage drops below a predetermined value. This state allows the batteries to recharge, while keeping the experiment "on" in a low power, non-operational condition. As the ni-cad batteries on the satellite developed their memory, the bus voltage dropped below the LVSF switched "off" for the first time since the launch in 1976. Numerous tests were run on the satellite to understand the problem and to check the state of the batteries. It was determined that the battery and solar cell capacity was as predicted, and most probably the battery memory was causing the LVSF trips.

Because the earth was near the maximum distance from the sun during this period, it was assumed (correctly) that the situation would improve over the subsequent months. NAG was instructed to minimize both the

total number of Doppler passes taken each week, and to maximize the ratio of sunlight/shadow passes in an attempt to maintain the battery in a higher state of charge. In addition, the experiment was turned "off" for one orbit each day. This mode of operation was used successfully until May 1978.

The reduced solar input to the solar cells (increased earth-sun distance), coupled with the ever-degrading battery, caused the LVSF switch to trip with ever-increasing frequency. Further study of the problem led to the decision to send the LVSF disable command that toggles the relay that deactivates the LVSF circuitry, thus enabling the boost regulator to gain access to the extra energy stored in the battery, but available only at a lower voltage. Careful management of the various commands was necessary to prevent a complete discharge of the battery. An operating procedure was developed that required NAG to communicate with the satellite on a daily basis, sending appropriate Doppler transmitter on/off, experiment on/off, and LVSF enable/disable commands. This operating mode resulted in the experiment being turned on approximately 16 hours a day, Monday through Friday, and turned off the remainder of the time. That mode was used successfully until August 1979. On a pass in which NAG was supposed to send commands to the satellite, no response from the spacecraft was obtained. On a subsequent pass over California, NAG was able to obtain telemetry information, although it was not of a quality to allow automatic data processing. Subsequent manual data analysis revealed that the buss voltage was about half of what it should have been, and that <u>both</u> the Doppler transmitter and the Wideband experiment were "on"--a condition that was never supposed to occur. Review of the command history revealed that no incorrect commands had been given, and that the spacecraft had responded correctly to all commands sent.

On several subsequent passes on several different days, commands were sent to turn the experiment "off"--all without result. This left the satellite in a condition that was certain to discharge the batteries completely. About a week later, while attempting to communicate with an operational TRANSIT satellite, NAG found the P76-5 satellite in a

normal condition with the Doppler transmitters "on" and the experiment in the low voltage condition! The experiment was commanded "on" and found to be operating properly. Tests conducted over the next few passes revealed that the batteries had degraded to the point that they could no longer provide adequate energy to get through the earth's shadow with the experiment turned "on." On a subsequent pass, the boost regulator failed to respond to a command to turn the experiment "on." It can only be concluded, therefore, that the LVSF portion of the boost regulator circuitry (or its associated command relay) failed, and caused the battery to be completely discharged, greatly reducing the battery capacity. It has also become impossible to reliably command the satellite.

It appears that further efforts to stretch the mission would be futile. The satellite has been left in a condition with the experiment in the low power (non-operational) mode with the Doppler transmitters "on." This provides the capability of Doppler tracking, telemetry decoding, and provides 150/400 MHz phase-coherent transmissions (without the normal TRANSIT modulation) for anyone who desires to receive them. Considering the fact that the original mission requirement was for a six months mission, with hopes for one year, the 3-1/2 years of continuous data gathering makes the Wideband experiment an extremely successful program.

REFERENCES

Basu, S., J. P. Mullen, and A. Bushty, "Long-Term 1.5 GHz Amplitude Scintillation Measurements at the Magnetic Equator," Geophys. Res. Lett., Vol. 7, No. 4, p. 259 (1980).

Chaturvedi, P. K. and S. L. Ossakow, "Nonlinear Stabilization of the Current Convective Instability in the Diffuse Aurora," Geophys. Res. Lett., Vol. 6, No. 12, p. 957 (1979).

Crane, R., "Spectra of Ionospheric Scintillation," J. Geophys. Res., Vol. 81, p. 2041 (1976).

Fremouw, E. J., C. L. Rino, and R. C. Livingston, "A Two-Component Model for Scintillation," in Proc. Symp. Cospar Satellite Beacon Group, 1-4 June 1976, Boston Univ., Boston, MA (1976).

Fremouw, E. J., C. L. Rino, R. C. Livingston, and M. C. Cousins, "A Persistent Subauroral Scintillation Enhancement Observed in Alaska," Geophys. Res. Letts., Vol. 4, p. 539 (1977).

Fremouw, E. J., R. L. Leadabrand, R. C. Livingston, M. D. Cousins, C. L. Rino, B. C. Fair, and R. A. Long, "Early Results from the DNA Wideband Satellite Experiment--Complex-Signal Scintillation," Radio Science, Vol. 13, p. 167 (1978).

Fremouw, E. J., R. C. Livingston, and D. A. Miller, "On the Statistics of Scintillating Signals," accepted for publication (1980).

Johnson, S. C. and C. L. Rino, "Binary Error Rates for a Two-Component Scintillation Channel," DNA 5071T, Topical Report 3, Contract DNA001-77-C-0038, SRI Project 5960, SRI International, Menlo Park, CA (August 1979).

Livingston, R. C., "Comparison of Multifrequency Equatorial Scintillation: American and Pacific Sectors," Radio Sci., Vol. 15, No. 4, p. 815 (1980).

Livingston, R. C., C. L. Rino, J. P. McClure, and W. B. Hanson, "Spectral Characteristics of Medium-Scale Equatorial F-Region Irregularities," J. Geophys. Res., submitted for publication (1980).

Ossakow, S. L., "Ionospheric Irregularities," Rev. Geophys. Space Phys., Vol. 17, No. 4, p. 521 (1979).

Ossakow, S. L. and P. K. Chaturvedi, "Morphological Studies of Rising Equatorial Spread F Bubbles," J. Geophys. Res., Vol. 83, p. 2085 (1978).

Rino, C. L., "Transionospheric Radiowave Propagation and Signal Statistics," paper presented at AGARD Symposium on Propagation Effects in Space/ Earth Paths, London, UK, 12-16 May 1980a.

Rino, C. L., "Numerical Computations for a One-Dimensional Power-Law Phase Screen," Radio Science, Vol. 15, p. 41 (1980b).

Rino, C. L., "Propagation Modeling and Evaluation of Communication System Performance in Nuclear Environments," DNA 5265F, Final Report, Contract DNA001-77-C-0038, SRI Project 5960, SRI International, Menlo Park, CA (February 1980c).

Rino, C. L., "A Power-Law Phase Screen Model for Ionospheric Scintillation 1. Weak Scatter," Radio Science, Vol. 14, No. 6, p. 1135 (1979a).

Rino, C. L., "A Power-Law Phase Screen Model for Ionospheric Scintillation 2. Strong Scatter," Radio Science, Vol. 14, No. 6, p. 1147 (1979b).

Rino, C. L. "Some Ramifications of the Power-Law Spectral Index," DNA 5078T, Topical Report 4, Contract DNA001-77-C-0038, SRI Project 5960, SRI International, Menlo Park, CA (October 1979c).

Rino, C. L. and E. J. Fremouw, "The Angle Dependence of Singly Scattered Wavefields," J. Atmos. Terr. Phys., Vol. 39, p. 859 (1977).

Rino, C. L. and R. C. Livingston, "A Spaced-Receiver Data Analysis Technique for Simultaneously Estimating Anisotropy and Pattern Drifts in Radio Wave Transmission Experiment," DNA 4792T, Topical Report 4, Contract DNA001-77-C-0220, SRI Project 6434, SRI International, Menlo Park, CA (1978).

Rino, C. L. and S. J. Matthews, "On the Morphology of Auroral-Zone Radiowave Scintillation," J. Geophys. Res., accepted for publication (1980).

Rino, C. L. and J. Owen, "The Time Structure of Transionospheric Radiowave Scintillation," Radio Sci., Vol. 15, No. 3, pp. 479-489 (1980a).

Rino, C. L. and J. Owen, "On the Temporal Coherence Loss of Strongly Scintillating Signals," Radio Science, submitted for publication (1980b).

Rino, C. L. and J. Owen, "The Structure of Localized Nighttime Auroral-Zone Scintillation Enhancements," J. Geophys. Res., Vol. 85, No. A6, p. 2941 (1980c).

Rino, C. L., V. H. Gonzalez, and A. R. Hessing, "Coherence Bandwidth Loss in Transionospheric Radio Propagation," Radio Science, submitted for publication (1980a).

Rino, C. L., R. T. Tsunoda, J. Petriceks, R. C. Livingston, M. C. Kelley, and D. K. Baker, "Simultaneous Rocket-Borne Beacon and In-Situ Measurements of Equatorial Spread F," J. Geophys. Res., submitted for publication (1980b).

Rino, C. L., E. J. Fremouw, R. C. Livingston, M. D. Cousins and B. C. Fair, "Wideband Satellite Observations," DNA 4399F, Final Report, Contract DNA001-75-C-0111, SRI Project 3793, SRI International, Menlo Park, CA (1977).

Scott, R. C. and D. L. Knepp, "Comparison of Signal Scintillation Models," Topical Report for February 1978 to June 1978, DNA 4652T, Contract DNA001-77-C-0096, Mission Research Corp., Santa Barbara, CA (1978).

Tsunoda, R. T., M. J. Baron, and J. Owen, "ALTAIR: An Incoherent Scatter Radar for Equatorial Spread-F Studies," DNA 4538T, Topical Report 1, Contract DNA001-77-C-0220, SRI Project 6434, SRI International, Menlo Park, CA (1978).

Vickrey, J. F., C. L. Rino, and T. A. Potemra, "Chatanika/TRIAD Observations of Unstable Ionization Enhancements in the Auroral F-Region," Geophys. Res. Letts., submitted for publication (1980).

Wittwer, L. A., "Transionospheric Signal Specifications for Satellite C^3 Applications," DNA/RAAE Technical Note, Washington, D.C. 20305 (20 March 1980).

Appendix A

WIDEBAND MAGNETIC TAPE FORMATS

There are three levels of tapes in the Wideband library; raw tapes of unprocessed data, detrend tapes of data prepared for analysis, and summary tapes of accumulated signal statistics. The formats of each of these tapes is described here. All are 9-track 1600-bpi density.

Raw Tapes

As outlined in Section II, thirteen complex channels of data for a single satellite pass are included on each raw tape recorded in the field. The file format of these tapes is shown in Figure 3. In addition to the main data file, a short initial file includes calibration data for the A-D converter. The last two files on the tape are RF calibrations. One is recorded system/sky noise with the receiver unlocked; the second is a constant-level coherent calibration signal.

Each record of the raw tape includes 50 ms of data and is 742, 16-bit-words long. All words are in standard Hewlett-Packard binary integers. The contents of each record are shown in Table 4. At Ancon (with a single-spaced receiver baseline) and at Stanford (with none), other channels are duplicated into the channels allocated for spaced receivers. Note also that the header portion of each record is different for the ADC calibration records.

Detrend Tapes

Of the 13 complex channels on the raw tapes, up to nine are decimated to 100 Hz and processed onto detrend tapes. The nine processed channels are split, three to a file, as shown in Figure 4. The channel allocations in each file are given in Table 5. At Stanford, where only six channels are processed, File 3 is zero-length. The remaining two

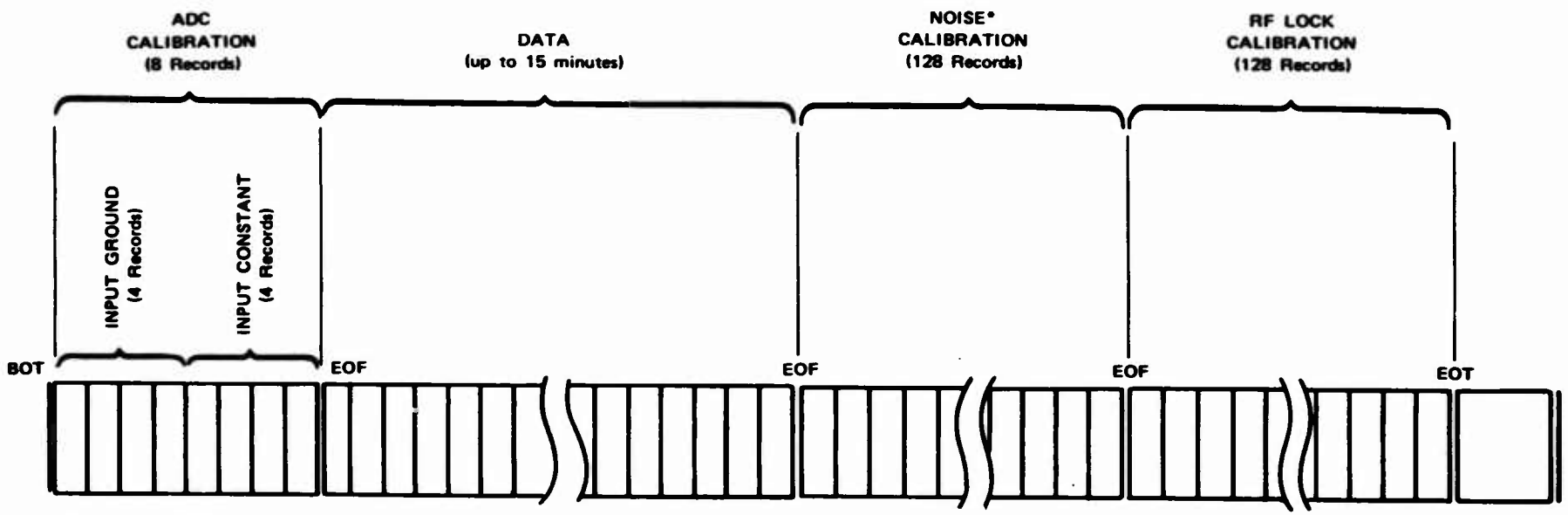

*ON SOME TAPES, ALL FILE MARKS OTHER THAN DATA MAY BE MISSING. ON NORMAL TAPES RECORDED BEFORE OCTOBER 1976, THE NOISE CALIBRATION FILE WILL BE MISSING.

FIGURE 3 WIDEBAND RAW TAPE FILE/RECORD STRUCTURE

Table 4

WIDEBAND RAW TAPE RECORD CONTENTS

The first 650 words of each 742-word record are data from the A/D input. The 650-word array is made up of 25 sequential groups of 26 words which are the sample values from the 13 pairs of channels in order. X-Y pairs are simultaneously sampled. Adjacent channels are samples 80 μs apart. The high-order 4 bits of each word is the channel number.

Word	Parameter
1 2	X* Y* 137.6748 MHz
3 4	X Y 413.0244 MHz--300-m west antenna (Poker Flat, Kwajalein)
5 6	X Y 413.0244 MHz--600-m east antenna (Poker Flat, Kwajalein, Ancon)
7 8	X Y 413.0244 MHz--900-m south antenna (Poker Flat, Kwajalein)
9 10	X Y 378.6057 MHz
11 12	X Y 390.0786 MHz
13 14	X Y 401.5515 MHz
15 16	X Y 413.0244 MHz
17 18	X Y 424.4973 MHz
19 20	X Y 435.9702 MHz
21 22	X Y 447.4431 MHz
23 24	X Y 1239.073 MHz
25 26	X Y 2891.171 MHz
27-650	Sequence of words 1 to 26 is repeated 25 times.

The remaining 92 words of each record is header information. For the data file, it contains the following information useful to outside users:

651-659	N/A
660	Hour
661	Minute
662	Second
663	Packed fraction of second
664	N/A
665	Day of year (BCD from clock)
666	N/A
667	Azimuth position from antenna controller (θ_x at Poker Flat)
668	Elevation position from antenna controller (θ_y at Poker Flat)
669-674	N/A
675	Azimuth position command (θ_x at Poker Flat)
676-679	N/A
680	Elevation position command (θ_y at Poker Flat)
681-687	N/A
688-690	Blank
691-706	N/A

*X = in-phase component, Y = phase quadrature component.

Table 4 (Concluded)

Word	Parameter
707-741	Blank
742	Record number

The header information for the first (ADC calibration) file is different. Those 8 records contain the following header data:

651-652	ADC calibration voltage applied (real word format)
653-660	N/A
661-680	ACSII data, first line of ephemeris message (20A2 format)*
681-700	ASCII data, second line of ephemeris message (20A2 format)*
701-742	N/A

*Only on records 1, 3, 5, and 7.

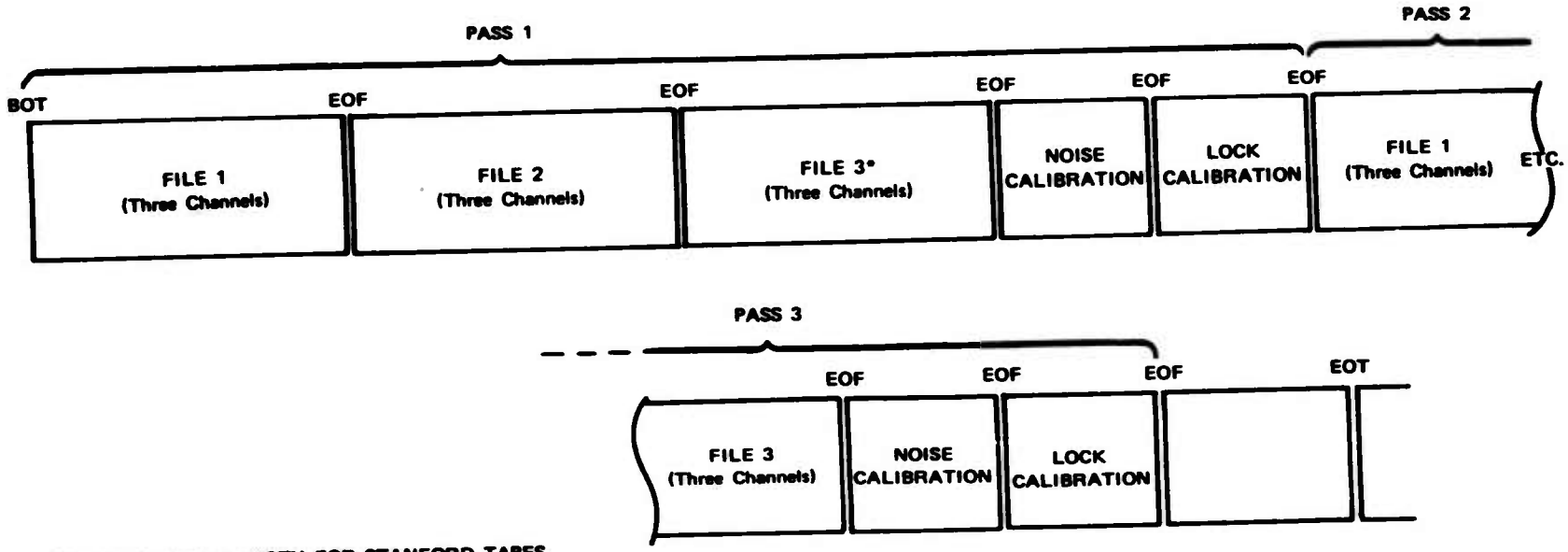

*FILE 3 IS ZERO-LENGTH FOR STANFORD TAPES.

FIGURE 4 WIDEBAND DETREND TAPE FILE STRUCTURE

Table 5

WIDEBAND DETREND TAPE
FILE/CHANNEL ALLOCATIONS

File	Channel		
	1	2	3
Poker Flat/Kwajalein			
1	137.7	378.6	447.5
2	2891.2	413.0	413.0 south
3	1239.1	413.0 east	413.0 west
Ancon			
1	137.67	378.6	447.5
2	2891.2	413.0	413.0 east
3	1239.1	390.1	436.0
Stanford			
1	137.67	378.6	447.5
2	2891.2	413.0	1239.1

files for each satellite pass are simply duplicates of the raw-tape RF calibration files. Usually three satellite passes, five files each, are included on a single tape.

Within each data file, the contents of each record are given in Table 6. Each record is 742 16-bit-words long, but includes a mixture of HP integrated real binary words. The first two records are copies of raw tape records 1 and 5, to carry over ADC calibration information. The remaining records (up to about 1600 of them) include 0.5 s of both rapidly and slowly varying detrend processing components, and header information.

Table 6

WIDEBAND DETREND FILE/RECORD CONTENTS

Record	Word No.	Parameter
1	1-742	Duplicate of raw tape record No. 1 (ADC ground)
2	1-742	Duplicate of raw tape record No. 5 (ADC constant voltage)
3	1	Intensity, Channel 1 — Detrended signal, i.e., components > 0.1 Hz, floating point words at 100 Hz rate; intensity: relative units unity mean; phase (dispersive Doppler): radians, continuous
	3	Phase, Channel 1
	5	Intensity, Channel 2
	7	Phase, Channel 2
	9	Intensity, Channel 3
	11	Phase, Channel 3
	13-600	Repeat (50 times) of above sequence
	601	Intensity, Channel 1 — Detrend reference signal, i.e., components < 0.1 Hz, floating point words at 20 Hz rate; intensity: scaled counts, 0 to $(2048)^2$; phase (dispersive Doppler): radians, continuous
	603	Phase, Channel 1
	605	Intensity, Channel 2
	607	Phase, Channel 2
	609	Intensity, Channel 3
	611	Phase, Channel 3
	613-720	Repeat (10 times) of above sequence
	721	Hour (integer)
	722	Minute (integer)
	723	Second (integer)
	724	Packed fraction of seconds
	725	N/A
	726	Day of year (BCD from clock)
	727	N/A
	728	Azimuth position from antenna controller (θ_x for Poker Flat)
	729	Elevation position from antenna controller (θ_y for Poker Flat)
	730	N/A
	731	N/A
	732	N/A
	733	N/A
	734	N/A
	735-742	Blank
4 through file mark		Repeat of record 3 format, each record corresponding to 0.5 seconds of data.

Summary Tapes

The summary tapes are a statistical condensation of the Wideband temporal data included on the detrend tapes. Unlike the raw and detrend binary tapes, the summaries are coded ASCII to simplify transfer to other computers.

Figure 5 shows the file and record structure of the summary tapes. Each tape starts with a file mark and contains data from 10 to 12 Wideband satellite passes, one file each. Each file, in time, starts with a header block four records long, followed by up to 45 data blocks. The formats of these records are outlined in Table 7, using the same notations used in Fremouw et al. [1978].

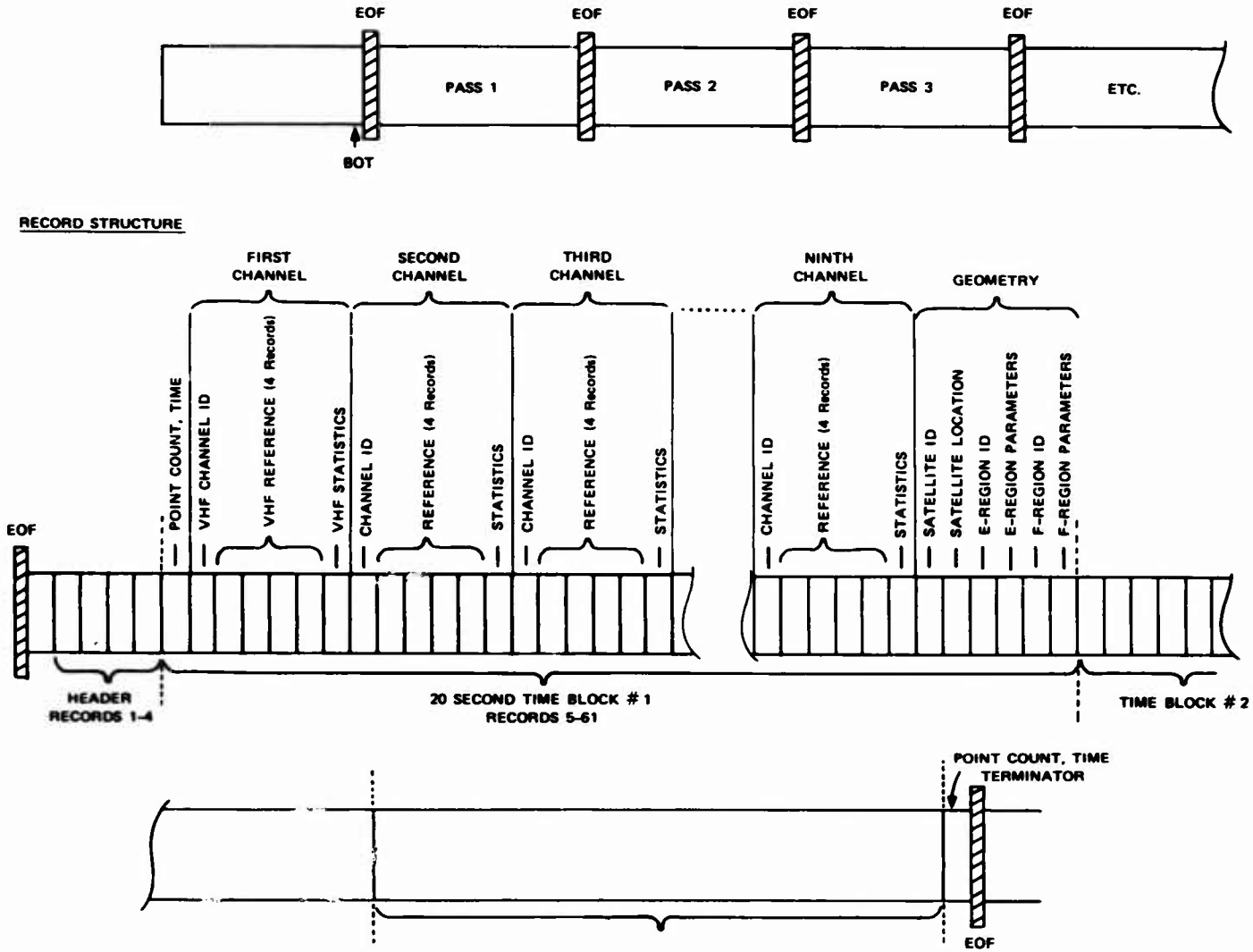

FIGURE 5 WIDEBAND SUMMARY TAPE FILE AND RECORD STRUCTURE

Table 7

SUMMARY TAPE CONTENTS

HEADER SECTION (First Four Records of Each Pass)		
Record	Format	Parameter
1	20A2	Station label
2	20A2	Blanks
3	3F10.4	Data detrend period (seconds, = 10 for Wideband)
		Year modulo 100
		Station number (1 = Poker Flat 2 = Stanford 3 = Ancon 4 = Kwajalein)
4	2(I3,4I2)	Day, Hour, Minute, Second, Millisecond — Start time of pass
		Day, Hour, Minute, Second, Millisecond — End time of pass

20-SECOND SUMMARY BLOCKS (Up to 45 per Pass Following Header Section)			
1	2I2,I3,4E2	Current data point counter	
		Total point counter in pass	
		Day, Hour, Minute, Second, Milliseconds — Current time, center of 20-second segment	
Note: Termination of the pass is indicated by all -1s in this record.			
2	2I2	Channel identifier = 1, 137.6748	
		Channel identifier = All stations	
3	10F10.4	Intensity (relative), Phase (rad) — Sample 1	VHF intensity and phase trends, i.e., components < 0.1 Hz, 1 Hz sampling rate
		Intensity, Phase — Sample 2	
		. . .	
		Intensity, Phase — Sample 5	
4	10F10.4	As record 3, samples 6-10	
5	10F10.4	As record 3, samples 11-15	
6	10F10.4	As record 3, samples 16-20	
7	9F10.4	S4 intensity scintillation index rms phase deviation (rad) Spectral slope of phase, P, 0.5 to 10 Hz rms least-squares fit, phase spectrum Spectral strength of phase, T, (dB mks units) Scintillation rate parameter, ν_c (Hz)	Statistics for VHF intensity and phase scintillation components, i.e., > 0.1 Hz

Table 7 (Continued)

Record	Format	Parameter
7 (Cont.)	9F10.4	rms least-squares cubic fit to intensity spectrum, 0.2 to 5.0 Hz Spectral slope of intensity 5 to 40 Hz Spectral strength of intensity (dB mks units)* } Statistics for VHF incensity and phase scintillation components, i.e., > 0.1 Hz
8	2I2	Channel identifier = 2, 413.0244 west, Poker Flat, Kwajalein Channel identifier = 3, 413.0244 east, Ancon = 5, 378.6057, Stanford
9-12	10F10.4	As records 3-6, trend components
13	9F10.4	As record 7, statistics
14	2I2	Channel identifier = 3, 413.0244 east, Poker Flat, Kwajalein Channel identifier = 5, 388.6057, Ancon = 8, 413.0244, Stanford
15-18	10F10.4	As records 3-6, trend components
19	9F10.4	As record 7, statistics
20 21-24 25		Channel identifier = 4, 413.0244 MHz south, Poker Flat, Kwajalein Channel identifier = 6, 390.0786 MHz, Ancon = 11, 447.4431 MHz, Stanford
26 27-30 31	2I2	Channel identifier = 5, 378.6057 MHz, Poker Flat, Kwajalein Channel identifier = 8, 413.0244, Ancon = 12, 1239.073, Stanford
32 33-36 37	2I2 10F10.4 9F10.4	Channel identifier = 8, 413.0255 MHz, Poker Flat, Kwajalein Channel identifier = 10, 435.9702 MHz, Ancon = 12, 1239.073 MHz, Stanford
38 39-42 43	2I2 10F10.4 9F10.4	Channel identifier = 11, 447.4431 MHz, Poker Flat, Kwajalein Ancon Channel identifier = 12, 1239.073 MHz, Stanford
44 45-48 49	2I2 10F10.4 9F10.4	Channel identifier Channel identifier = 12, 1239.073 MHz, all stations
50 51-54 55	2I2 10F10.4 9F10.4	Channel identifier Channel identifier = 13, 2891.171 MHz, all stations
56	2I2	Satellite location identifier (= 20) Satellite location identifier (= 20)
57	13F8.3	Azimuth angle, station to satellite (deg)
		Elevation angle, station to satellite (deg)
		Satellite latitude (deg, +N)
		Satellite longitude (deg, +E)
		Satellite height (km)
		(Zero)
		(Zero)
		(Zero)
		(Zero)
		(Zero)
		(Zero)
		(Zero)
		(Zero)

*On early tapes, this parameter is the rms least-squares linear fit to the intensity spectrum 5 to 40 Hz.

Table 7 (Concluded)

Record	Format	Parameter
58	2I2	E-region (110 km) penetration point identifier (= 21) E-region (110 km) penetration point identifier (= 21)
59	13F8.3	Penetration point latitude (deg, +N)
		Penetration point longitude (deg, +E)
		Penetration point height (= 110 km)
		Magnetic latitude (deg, +N)
		L-shell
		Dip angle (deg)
		Magnetic azimuth (deg)
		Zenith angle (deg)
		Briggs-Parkin angle (deg)
		Reduced propagation range (km)
		Scan velocity, x component (km/s)
		Scan velocity, y component (km/s)
		Scan velocity, z component (km/s)
60	2I2	F-region (350 km) penetration point identifier (= 22) F-region (350 km) penetration point identifier (= 22)
61	13F8.3	As record 29, but for 350 km penetration altitude
Continued repeat of data block records 1-61 for up to 45 data blocks		
Last record	2I2,I3,4I2	All -1s indicate end of pass

Appendix B

PUBLICATIONS RELATING TO WIDEBAND PROJECT

WIDEBAND SATELLITE (P76-5) PUBLICATIONS

Rino, C. L. and E. J. Fremouw, "The Angle Dependence of Singly Scattered Wavefields," J. Atmos. Terr. Phys., Vol. 39, p. 859 (1977).

Fremouw, E. J., C. L. Rino, R. C. Livingston, and M. C. Cousins, "A Persistent Subauroral Scintillation Enhancement Observed in Alaska," Geophys. Res. Letts., Vol. 4, No. 11, p. 539 (1977).

Rino, C. L., R. C. Livingston, M. D. Cousins, B. C. Fair, and M. J. Baron, "Amplitude and Phase Scintillation at High and Equatorial Latitudes as Measured by the DNA Wideband Satellite," paper presented at the IES Symposium on the Effect of the Ionosphere on Space Systems and Communications, Arlington, VA (January 1978).

Rino, C. L., C. H. Dawson, R. C. Livingston, and J. Petriceks, "The Ionospheric Limitation to Coherent Integration in Transionospheric Radars," paper presented at the IES Symposium on the Effect of the Ionosphere on Space Systems and Communications, Arlington, VA (January 1978).

Fremouw, E. J., R. L. Leadabrand, R. C. Livingston, M. D. Cousins, C. L. Rino, B. C. Fair, and R. A. Long, "Early Results from the DNA Wideband Satellite Experiment--Complex-Signal Scintillation," Radio Sci., Vol. 13, No. 1, p. 167 (1978).

Rino, C. L., "Radio-Wave Scintillation as Measured by the Wideband Satellite," paper presented at the National Telecommunications Conference, Birmingham, AL (December 1978).

Rino, C. L., R. C. Livingston, and S. J. Matthews, "Evidence for Sheet-Like Auroral Ionospheric Irregularities," Geophys. Res. Letts., Vol. 5, No. 12, p. 1039 (1978).

Rino, C. L., "A Power-Law Phase Screen Model for Ionospheric Scintillation 1. Weak Scatter," Radio Sci., Vol. 14, No. 6, p. 1135 (1979).

Tsunoda, R. T., M. J. Baron, J. Owen, and D. M. Towle, "ALTAIR: An Incoherent-Scatter Radar for Equatorial Spread-F Studies," Radio Sci., Vol. 14, No. 6, p. 1111 (1979).

Rino, C. L. and J. Owen, "The Time Structure of Transionospheric Radiowave Scintillation," Radio Sci., accepted for publication (1980).

Livingston, R. C., "Comparison of Multifrequency Equatorial Scintillation: American and Pacific Sectors," Radio Sci., Vol. 15, No. 4, p. 815 (1980).

Rino, C. L. and S. J. Matthews, "On the Morphology of Auroral-Zone Radiowave Scintillation," J. Geophys. Res., submitted for publication (1980).

Rino, C. L. and J. Owen, "The Structure of Localized Nighttime Auroral-Zone Scintillation Enhancements," J. Geophys. Res., submitted for publication (1980).

WIDEBAND SATELLITE (P76-5) REPORTS

Rino, C. L., E. J. Fremouw, R. C. Livingston, M. D. Cousins, and B. C. Fair, "Wideband Satellite Observations," Final Report for Period 26 May 1976-31 May 1977, DNA 4399F, Contract DNA001-75-C-0111, SRI Project 3793, SRI International, Menlo Park, CA (June 1977).

Rino, C. L., J. Petriceks, R. Livingston, and C. Dawson, "Data Reduction and Analysis of Coherent Satellite Transmissions," Final Report Covering the Period 2 June through 16 December 1977, Purchase Order No. 211-275012-40472, SRI Project 6449, SRI International, Menlo Park, CA (December 1977).

Tsunoda, R. T., M. J. Baron, and J. Owen, "ALTAIR: An Incoherent Scatter Radar for Equatorial Spread-F Studies," Topical Report 1 Covering the period 1 June 1977 to 1 January 1978, DNA 4538T, Contract DNA001-77-C-0220, SRI Project 6434, SRI International, Menlo Park, CA (January 1978).

Rino, C. L. and S. J. Matthews, "On the Interpretation of Ionospheric Scintillation Data Using a Power-Law Phase Screen Model--Weak Scatter," Topical Report 2 Covering 1 June 1977 to 28 February 1978, DNA 4606T, Contract DNA001-77-C-0220, SRI Project 6434, SRI International, Menlo Park, CA (February 1978).

Livingston, R. C., "Comparative Equatorial Scintillation Morphology--American and Pacific Sectors," Topical Report 3 Covering 1 June 1977 to 30 June 1978, DNA 4644T, Contract DNA001-77-C-0220, SRI Project 6434, SRI International, Menlo Park, CA (June 1978).

Rino, C. L. and R. C. Livingston, "A Spaced-Receiver Data Analysis Technique for Simultaneously Estimating Anisotropy and Pattern Drifts in Radio Wave Transmission Experiments," Topical Report 4 Covering 1 June 1977 to 30 September 1978, DNA 4792, Contract DNA001-77-C-0220, SRI Project 6434, SRI International, Menlo Park, CA (September 1978).

Rino, C. L., "Scintillation Structure in a Severely Disturbed Scattering Environment," Topical Report 2 Covering the Period 1 November 1977 to 30 September 1978, DNA 4732T, Contract DNA001-77-C-0038, SRI Project 5960, SRI International, Menlo Park, CA (October 1978).

Rino, C. L. and J. Owen, "The Temporal Structure of Strongly Scintillating Signals," Topical Report 5 Covering 1 August to 30 December 1978, DNA 4827T, Contract DNA001-77-C-0220, SRI Project 6434, SRI International, Menlo Park, CA (January 1979).

Matthews, S. J. and C. L. Rino, "High Latitude Scintillation Morphology--Alaskan Sector," Topical Report 6 Covering May 1976 to April 1978, DNA 5131T, Contract DNA001-77-C-0220, SRI Project 6434, SRI International, Menlo Park, CA (October 1979).

REPORTS RELATING TO WIDEBAND PROJECT

Rino, C. L., "Scintillation Structure in a Severely Disturbed Scattering Environment," Topical Report covering 1 November 1977 to 30 September 1978, DNA 4732T, SRI Project 5960, SRI International, Menlo Park, CA (1978).

Johnson, S. C. and C. L. Rino, "Binary Error Rates for a Two-Component Scintillation Channel," Topical Report for period 1 January 1979 to 31 August 1979, DNA 5071T, SRI Project 5960, SRI International, Menlo Park, CA (1979).

Rino, C. L., "Some Ramifications of the Power-Law Spectral Index for Propagation Modeling," Topical Report for period 1 January 1979 to 30 September 1979, DNA 5078T, SRI Project 5960, SRI International, Menlo Park, CA (1979).

Rino, C. L., "Propagation Modeling and Evaluation of Communication System Performance in Nuclear Environments," Final Report for period November 1976 through 29 February 1980, DNA 5265F, SRI Project 5960, SRI International, Menlo Park, CA (1980).

Rino, C. L., J. Petriceks, R. C. Livingston, and C. Dawson, "Data Reduction and Analysis of Coherent Satellite Transmissions," Final Report for period 2 June through 16 December 1977, Purchase Order No. 211-275012-40472, SRI Project 6449, SRI International, Menlo Park, CA (1977).

DISTRIBUTION LIST

DEPARTMENT OF DEFENSE

Assistant Secretary of Defense
Comm, Cmd, Cont & Intell
ATTN: Dir of Intelligence Systems, J. Babcock
ATTN: C3IST&CCS

Assistant to the Secretary of Defense
Atomic Energy
ATTN: Executive Assistant

Command & Control Technical Center
Department of Defense
ATTN: C-312, R. Mason
ATTN: C-650, G. Jones
3 cy ATTN: C-650, W. Heidig

Defense Communications Agency
ATTN: Code 205
ATTN: 810, J. Barna
ATTN: Code 480
ATTN: 101B
ATTN: Code 480, F. Dieter

Defense Communications Engineer Center
ATTN: Code R123
ATTN: Code R410, N. Jones

Defense Intelligence Agency
ATTN: DB-4C, E. O'Farrell
ATTN: HQ-TR, J. Stewart
ATTN: DB, A. Wise
ATTN: DT-5
ATTN: DT-1B
ATTN: DC-7D, W. Wittig

Defense Nuclear Agency
ATTN: RAEE
ATTN: STNA
ATTN: NATD
ATTN: NAFD
3 cy ATTN: RAAE
4 cy ATTN: TITL

Defense Technical Information Center
Cameron Station
12 cy ATTN: DD

Field Command
Defense Nuclear Agency
ATTN: FCPR

Field Command
Defense Nuclear Agency
Livermore Branch
ATTN: FCPRL

Interservice Nuclear Weapons School
ATTN: TTV

Joint Chiefs of Staff
ATTN: C3S
ATTN: C3S, Evaluation Office

Joint Strat Tgt Planning Staff
ATTN: JLA
ATTN: JLTW-2

DEPARTMENT OF DEFENSE (Continued)

National Security Agency
ATTN: W-32, O. Bartlett
ATTN: B-3, F. Leonard
ATTN: R-52, J. Skillman

Undersecretary of Def for Rsch & Engrg
Department of Defense
ATTN: Strategic & Space Sys (OS)

WWMCCS System Engineering Org
ATTN: R. Crawford

DEPARTMENT OF THE ARMY

Assistant Chief of Staff for Automation & Comm
Department of the Army
ATTN: DAAC-ZT, P. Kenny

Atmospheric Sciences Laboratory
U.S. Army Electronics R&D Command
ATTN: DELAS-EO, F. Niles

BMD Advanced Technology Center
Department of the Army
ATTN: ATC-O, W. Davies
ATTN: ATC-T, M. Capps

BMD Systems Command
Department of the Army
2 cy ATTN: BMDSC-HW

Deputy Chief of Staff for Ops & Plans
Department of the Army
ATTN: DAMO-RQC

Electronics Tech & Devices Lab
U.S. Army Electronics R&D Command
ATTN: DELET-ER, H. Bomke

Harry Diamond Laboratories
Department of the Army
ATTN: DELHD-N-P, F. Wimenitz
ATTN: DELHD-N-P
ATTN: DELHD-N-RB, R. Williams
ATTN: DELHD-I-TL, M. Weiner

U.S. Army Comm-Elec Engrg Instal Agency
ATTN: CCC-CED-CCO, W. Neuendorf
ATTN: CCC-EMEO-PED, G. Lane

U.S. Army Communications Command
ATTN: CC-OPS-WR, H. Wilson
ATTN: CC-OPS-W

U.S. Army Communications R&D Command
ATTN: DRDCO-COM-RY, W. Kesselman

U.S. Army Foreign Science & Tech Ctr
ATTN: DRXST-SD

U.S. Army Materiel Dev & Readiness Cmd
ATTN: DRCLDC, J. Bender

U.S. Army Missile Intelligence Agency
ATTN: J. Gamble

DEPARTMENT OF THE ARMY (Continued)

U.S. Army Nuclear & Chemical Agency
ATTN: Library

U.S. Army Satellite Comm Agency
ATTN: Document Control

U.S. Army TRADOC Sys Analysis Actvy
ATTN: ATAA-TDC
ATTN: ATAA-PL
ATTN: ATAA-TCC, F. Payan, Jr

DEPARTMENT OF THE NAVY

Joint Cruise Missiles Project
Department of the Navy
ATTN: JCMG-707

Naval Air Development Center
Johnsville
ATTN: Code 6091, M. Setz

Naval Air Systems Command
ATTN: PMA 271

Naval Electronic Systems Command
ATTN: PME-117-2013, G. Burnhart
ATTN: PME-106-13, T. Griffin
ATTN: Code 501A
ATTN: PME-117-211, B. Kruger
ATTN: Code 3101, T. Hughes
ATTN: PME-117-20
ATTN: PME-106-4, S. Kearney

Naval Intelligence Support Ctr
ATTN: NISC-50

Naval Ocean Systems Center
ATTN: Code 532, J. Bickel
ATTN: Code 5322, M. Paulson
3 cy ATTN: Code 5323, J. Ferguson
3 cy ATTN: Code 5324, W. Moler

Naval Research Laboratory
ATTN: Code 4780, S. Ossakow
ATTN: Code 7550, J. Davis
ATTN: Code 4187
ATTN: Code 4700, T. Coffey
ATTN: Code 7500, B. Wald

Naval Space Surveillance System
ATTN: J. Burton

Naval Surface Weapons Center
White Oak Laboratory
ATTN: Code F31

Naval Telecommunications Command
ATTN: 341

Office of Naval Research
ATTN: Code 420
ATTN: Code 465
ATTN: Code 421

DEPARTMENT OF THE NAVY (Continued)

Office of the Chief of Naval Operations
ATTN: OP 65
ATTN: OP 981N
ATTN: OP 941D

Strategic Systems Project Office
Department of the Navy
ATTN: NSP-43
ATTN: NSP-2141
ATTN: NSP-2722, F. Wimberly

DEPARTMENT OF THE AIR FORCE

Aerospace Defense Command
Department of the Air Force
ATTN: DC, T. Long

Air Force Geophysics Laboratory
ATTN: OPR, H. Gardiner
ATTN: OPR-1
ATTN: LKB, K. Champion
ATTN: OPR, A. Stair
ATTN: PHP
ATTN: PHI, J. Buchau

Air Force Weapons Laboratory
Air Force Systems Command
ATTN: SUL
ATTN: NTYC
ATTN: NTN

Air Force Wright Aeronautical Lab
ATTN: A. Johnson
ATTN: W. Hunt

Air Logistics Command
Department of the Air Force
ATTN: OO-ALC/MM, R. Blackburn

Air University Library
Department of the Air Force
ATTN: AUL-LSE

Assistant Chief of Staff
Intelligence
Department of the Air Force
ATTN: INED

Assistant Chief of Staff
Studies & Analyses
Department of the Air Force
ATTN: AF/SASC, G. Zank
ATTN: AF/SASC, W. Adams

Ballistic Missile Office
Air Force Systems Command
ATTN: MNNL, S. Kennedy
ATTN: MNNXH, J. Allen

DEPARTMENT OF THE AIR FORCE (Continued)

Deputy Chief of Staff
Operations Plans and Readiness
Department of the Air Force
ATTN: AFXOKT
ATTN: AFXOKCD
ATTN: AFXOXFD
ATTN: AFXOKS

Deputy Chief of Staff
Research, Development, & Acq
Department of the Air Force
ATTN: AFRDS
ATTN: AFRDSS
ATTN: AFRDSP

Electronic Systems Division
ATTN: DCKC, J. Clark

Electronic Systems Division
ATTN: XRW, J. Deas

Electronic Systems Division
ATTN: YSM, J. Kobelski
ATTN: YSEA

Foreign Technology Division
Air Force Systems Command
ATTN: TQTD, B. Ballard
ATTN: NIIS Library

Headquarters Space Division
Air Force Systems Command
ATTN: SKY, C. Kennedy
ATTN: SKA, D. Bolin

Headquarters Space Division
Air Force Systems Command
ATTN: YZJ, W. Mercer

Headquarters Space Division
Air Force Systems Command
ATTN: E. Butt

Rome Air Development Center
Air Force Systems Command
ATTN: OCS, V. Coyne
ATTN: TSLD

Rome Air Development Center
Air Force Systems Command
ATTN: EEP

Strategic Air Command
Department of the Air Force
ATTN: DCXR, T. Jorgensen
ATTN: DCXT
ATTN: NRT
ATTN: XPFS
ATTN: DCX

OTHER GOVERNMENT AGENCIES

Central Intelligence Agency
ATTN: OSWR/NED

Department of Commerce
National Bureau of Standards
ATTN: Sec Ofc for R. Moore

OTHER GOVERNMENT AGENCIES (Continued)

Department of Commerce
National Oceanic & Atmospheric Admin
ATTN: R. Grubb

Institute for Telecommunications Sciences
ATTN: W. Utlaut
ATTN: L. Berry
ATTN: D. Crombie
ATTN: A. Jean

U.S. Coast Guard
Department of Transportation
ATTN: G-DOE-3/TP54, B. Romine

DEPARTMENT OF ENERGY CONTRACTORS

EG&G, Inc
Los Alamos Division
ATTN: D. Wright
ATTN: J. Colvin

Lawrence Livermore National Lab
ATTN: L-31, R. Hager
ATTN: Technical Info Dept Library
ATTN: L-389, R. Ott

Los Alamos National Scientific Lab
ATTN: MS 670, J. Hopkins
ATTN: MS 664, J. Zinn
ATTN: D. Simons
ATTN: E. Jones
ATTN: D. Westervelt
ATTN: P. Keaton
ATTN: R. Taschek

Sandia National Laboratories
Livermore Branch
ATTN: T. Cook
ATTN: B. Murphey

Sandia National Lab
ATTN: Org 1250, W. Brown
ATTN: D. Thornbrough
ATTN: D. Dahlgren
ATTN: Space Project Div
ATTN: 3141
ATTN: Org 4241, T. Wright

DEPARTMENT OF DEFENSE CONTRACTORS

Aerospace Corp
ATTN: I. Garfunkel
ATTN: V. Josephson
ATTN: D. Olsen
ATTN: S. Bower
ATTN: J. Straus
ATTN: N. Stockwell
ATTN: T. Salmi
ATTN: R. Slaughter

University of Alaska
Geophysical Institute
ATTN: N. Brown
ATTN: T. Davis
ATTN: Technical Library

DEPARTMENT OF DEFENSE CONTRACTORS (Continued)

Analytical Systems Engineering Corp
ATTN: Radio Sciences

Analytical Systems Engineering Corp
ATTN: Security

Barry Research Corporation
ATTN: J. McLaughlin

BDM Corp
ATTN: L. Jacobs
ATTN: T. Neighbors

Berkeley Research Associates, Inc
ATTN: J. Workman

Betac
ATTN: J. Hirsch

Boeing Co
ATTN: G. Hall
ATTN: S. Tashird
ATTN: M/S 42-33, J. Kennedy

Booz-Allen & Hamilton, Inc
ATTN: B. Wilkinson

University of California at San Diego
Electronical Engineering Computer Sciences
ATTN: H. Booker

Charles Stark Draper Lab, Inc
ATTN: D. Cox
ATTN: J. Gilmore

Computer Sciences Corp
ATTN: H. Blank

Comsat Labs
ATTN: R. Taur
ATTN: G. Hyde

Cornell University
Department of Electrical Engineering
ATTN: M. Kelly
ATTN: D. Farley, Jr

Electrospace Systems, Inc
ATTN: H. Logston

ESL, Inc
ATTN: J. Marshall

General Electric Co
Space Division
Valley Forge Space Center
ATTN: A. Harcar
ATTN: M. Bortner

General Electric Co
Re-Entry Systems Division
ATTN: C. Zierdt
ATTN: A. Steinmayer

General Electric Co
ATTN: F. Reibert

DEPARTMENT OF DEFENSE CONTRACTORS (Continued)

General Electric Tech Services Co, Inc
Electronic Park
ATTN: G. Millman

General Research Corp
Santa Barbara Division
ATTN: J. Garbarino
ATTN: J. Ise, Jr

HSS, Inc
ATTN: D. Hansen

IBM Corp
Federal Systems Division
ATTN: F. Ricci

University of Illinois
ATTN: Security Supervisor for K. Yeh

Institute for Defeense Analyses
ATTN: J. Bengston
ATTN: H. Wolfhard
ATTN: J. Aein
ATTN: E. Bauer

International Tel & Telegraph Corp
ATTN: G. Wetmore
ATTN: Technical Library

Jaycor
ATTN: J. Sperling

Jaycor
ATTN: J. Doncarlos

Johns Hopkins University
Applied Physics Lab
ATTN: P. Komiske
ATTN: T. Potemra
ATTN: T. Evans
ATTN: J. Newland
ATTN: J. Phillips

Kaman TEMPO
ATTN: T. Stephens
ATTN: D. Chandler
ATTN: M. Stanton
ATTN: DASIAC
ATTN: W. Knapp
ATTN: W. McNamara

Linkabit Corp
ATTN: I. Jacobs

Litton Systems, Inc
Amecom Division
ATTN: R. Grasty

Lockheed Missiles & Space Co, Inc
ATTN: W. Imhof
ATTN: R. Johnson
ATTN: M. Walt

Lockheed Missiles & Space Co, Inc
ATTN: D. Churchill
ATTN: Dept 60-12

DEPARTMENT OF DEFENSE CONTRACTORS (Continued)

M.I.T. Lincoln Lab
ATTN: L. Loughlin
ATTN: D. Towle

Martin Marietta Corp
ATTN: R. Heffner

McDonnell Douglas Corp
ATTN: W. Olson
ATTN: R. Halprin
ATTN: G. Mroz
ATTN: N. Harris
ATTN: J. Moule

Meteor Communications Consultants
ATTN: R. Leader

Mission Research Corp
ATTN: R. Hendrick
ATTN: F. Fajen
ATTN: Tech Library
ATTN: D. Sappenfield
ATTN: R. Kilb
ATTN: S. Gutsche
ATTN: R. Bogusch

Mitre Corp
ATTN: B. Adams
ATTN: C. Callahan
ATTN: G. Harding
ATTN: A. Kymmel

Mitre Corp
ATTN: J. Wheeler
ATTN: W. Foster
ATTN: M. Horrocks
ATTN: W. Hall

Pacific-Sierra Research Corp
ATTN: E. Field, Jr
ATTN: F. Thomas
ATTN: H. Brode

Pennsylvania State University
ATTN: Ionospheric Research Lab

Photometrics, Inc
ATTN: I. Kofsky

Physical Dynamics, Inc
ATTN: E. Fremouw

R & D Associates
ATTN: W. Karzas
ATTN: M. Gantsweg
ATTN: F. Gilmore
ATTN: W. Wright
ATTN: C. Greifinger
ATTN: B. Gabbard
ATTN: R. Turco
ATTN: H. Ory
ATTN: R. Lelevier
ATTN: P. Haas

R & D Associates
ATTN: B. Yoon
ATTN: L. Delaney

DEPARTMENT OF DEFENSE CONTRACTORS (Continued)

Rand Corp
ATTN: E. Bedrozian
ATTN: C. Crain

Riverside Research Institute
ATTN: V. Trapani

Rockwell International Corp
ATTN: R. Buckner

Rockwell International Corp
Collins Telecommunications Sys Division
ATTN: S. Quilici

Sante Fe Corp
ATTN: D. Paolucci

Science Applications, Inc
ATTN: C. Smith
ATTN: D. Hamlin
ATTN: L. Linson
ATTN: E. Straker

Science Applications, Inc
ATTN: SZ

Science Applications, Inc
ATTN: J. Cockayne

SRI International
ATTN: G. Price
ATTN: A. Burns
ATTN: J. Petrickes
ATTN: R. Tsunoda
ATTN: M. Baron
ATTN: R. Leadabrand
ATTN: D. Neilson
ATTN: G. Smith
ATTN: W. Jaye
ATTN: W. Chesnut
4 cy ATTN: B. Fair
4 cy ATTN: M. Cousins
4 cy ATTN: R. Livingston
10 cy ATTN: C. Rino

Sylvania Systems Group
Communication Systems Division
ATTN: M. Cross

Technology International Corp
ATTN: W. Boquist

Tri-Comm, Inc
ATTN: D. Murray

TRW Defense & Space Sys Group
ATTN: D. Dee
ATTN: R. Plebuch

Utah State University
ATTN: J. Dupnik
ATTN: K. Baker
ATTN: L. Jensen

Visidyne, Inc
ATTN: J. Carpenter
ATTN: C. Humphrey